NANO LETTERS

2008
Vol. 8, No. 1
168−172

Highly Responsive Hydrogel Scaffolds Formed by Three-Dimensional Organization of Microgel Nanoparticles

Eun Chul Cho,[†,||] Jin-Woong Kim,[†,‡,||] Alberto Fernández-Nieves,[‡,§] and David A. Weitz*[,‡]

Amore-Pacific Company Research and Development Center, 314-1, Bora-dong, Giheung-gu, Yongin-si, Gyeonggi-Do, 446-729, Korea, and Harvard School of Engineering and Applied Sciences and Department of Physics, Harvard University, Cambridge, Massachusetts 02138

Received September 12, 2007; Revised Manuscript Received December 1, 2007

ABSTRACT

We present a robust and straightforward method for fabricating remarkably responsive hydrogel scaffolds consisting of submicron-sized microgel particles. We demonstrate that the microgel particles assemble either through bridging or depletion interactions to yield a structure that swells or deswells at a macroscopic level in much shorter times as compared to a bulk polymer gel of similar characteristics. This approach offers a new way of fabricating functional hydrogel scaffolds with controllable responsiveness to applied stimuli and excellent loading capability for a wide variety of materials, irrespective of chemistry, size, and shape.

Stimuli-responsive hydrogels can swell or deswell in response to changes in external triggers such as pH,[1] temperature,[2] electric fields,[3] light,[4−7] and biomolecules;[8] this makes them useful for fundamental studies as well as industrial applications in fields such as drug delivery,[9−12] nanopatterning,[13] chemical and biosensing,[14,15] and photonic crystals.[16−18] However, typically their response is not sufficiently fast to make them widely useful, because the swelling kinetics is determined by the relaxation of the polymer network, which is proportional to the square of the gel size.[19,20] Moreover, the response is even slower if the swelling is accompanied by phase separation stemming from spinodal decomposition,[21−23] which usually occurs on length scales of $\sim 1\ \mu$m. Although there have been efforts to improve the response kinetics by using sophisticated techniques that incorporate additional porosity into the hydrogel[24−26] or achieve either grafting of dangling chains[27,28] or hybridizing nanoparticles[29,30] within the polymer network, there is still no proven method to fabricate a polymer gel with a fast response time on macroscopic length scales.

In this letter, we report a method for making thermally responsive hydrogel scaffolds with a remarkably rapid response to temperature changes. The procedure is based on the aggregation and subsequent colloidal gelation of submicron-sized microgel particles at room temperature; this is achieved by using free polymers that either bridge or induce a depletion attraction between the microgel particles. The colloidal gel structure is then chemically treated at higher temperatures to create covalent bonds between the microgel particles, as shown schematically in Figure 1a, thereby producing a mesoporous three-dimensional (3D) hydrogel scaffold. The advantages of this technique include the possibility of obtaining hydrogel scaffolds with different shapes that exhibit remarkably fast response to changes in temperature. In addition, our method is very flexible and enables immobilization of both biomolecules and colloidal materials of different types and sizes within the network of microgel particles, because the clustering process can occur in the presence of added materials.

In a typical procedure, we use ∼800 nm poly(*N*-isopropylacrylamide) (PNIPAm) microgel particles as building blocks (See Supporting Information, Figure 1b). To add both interaction and reaction sites onto the microgel particles, we copolymerize ∼5 mol % allylamine with NIPAm monomers; this adds amine groups, which dissociate to yield ammonium ions. Successful incorporation of these positive charges into the microgel particles can be confirmed by measuring the electrophoretic mobility of the particles, which is $\sim 1.5 \times 10^{-8}$ m^2 V^{-1} s^{-1}. We then add a long water-soluble polymer, poly(acrylic acid) (PAAc), to the microgel dispersion inside a glass vial. This induces the formation of microgel

* Corresponding author. Tel: 617-496-2842. Fax: 617-495-2875. E-mail: weitz@seas.harvard.edu.
† Amore-Pacific Company Research and Development Center.
‡ Harvard University.
§ Present address: School of Physics, Georgia Institute of Technology, Atlanta, Georgia 30332.
|| These authors contributed equally to this work.

10.1021/nl072346e CCC: $40.75
Published on Web 12/18/2007

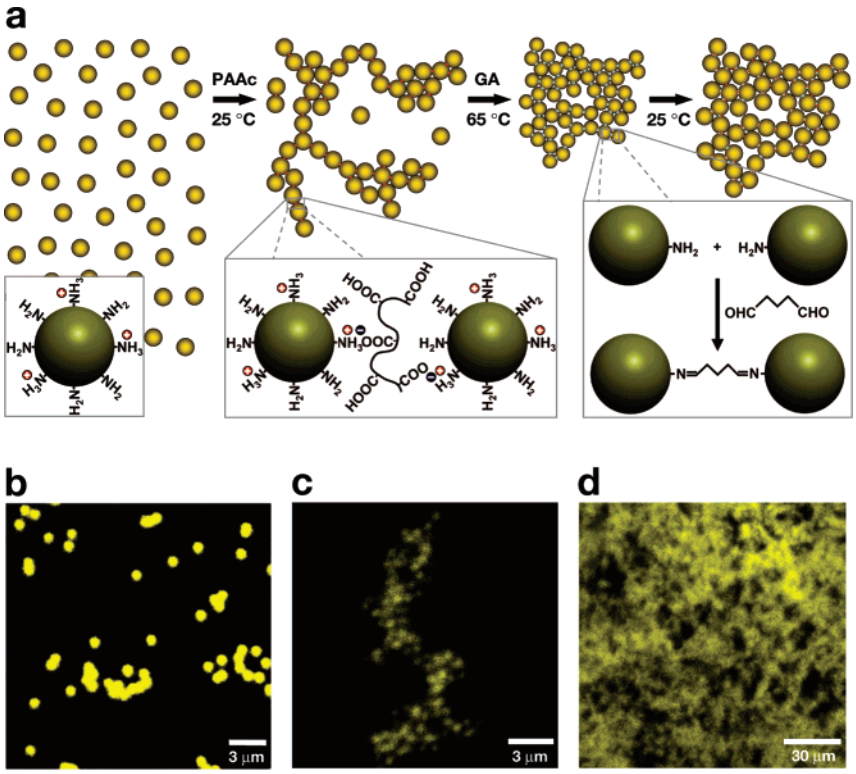

Figure 1. The process for fabricating stimuli-responsive hydrogel scaffolds. (a) Schematic for the controlled aggregation and colloidal gelation of the microgel particles. (b) Initially the microgel particles dispersed in water were positively charged due to the partial dissociation of amine groups on their surface. (c) A cluster consisting of microgel particles formed after inducing the electrostatic attraction between the positively charged microgel particles and the negatively charged poly(acrylic acid). After the cluster grew and formed a colloidal gel, the sample was heated to bring the microgel particles close to each other. Then glutaldehyde was added to covalently link them. (d) The fabrication process resulted in a 3D responsive microgel scaffold. These microgel particles labeled by copolymerizing with a fluorescence monomer, methacryloxy thiocarbonyl rhodamine B (0.01 wt %, Polyfluor 570, Polysciences) were observed by using a confocal laser scanning microscope (Zeiss).

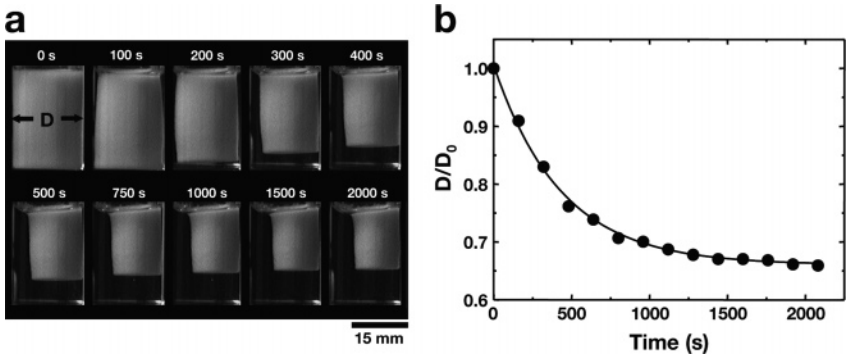

Figure 2. The heating process of the microgel particle-based colloidal gel. (a) Time series of the heating process. The temporal origin was chosen when a 5 mL glass vial containing the colloidal gel structure is placed inside a glycerol bath at 65 °C. (b) Phase change kinetics of the colloidal gel as a function of time at 65 °C. Diameter of the cylindrical hydrogel, D, was normalized with the initial diameter, D_0.

clusters due to a polymer-mediated bridging process, which results from the electrostatic attraction between the ammonium ions of the microgel particles and the carboxyl groups of the PAAc[31,32] (Figure 1c). These clusters grow in size to form a colloidal gel that spans the space of the container; this provides a definite shape to the gel structure. The process is finished by heating the gel structure to induce its shrinkage and compaction, then adding glutaldehyde to covalently link the microgel particles together.[33] The final result is a stable 3D hydrogel scaffold, as shown in Figure 1d.

The heating step of the fabrication process is shown in detail in Figure 2a (see also Supporting Information, movie S1). A feature of this process is that the structure retains the cylindrical shape of the container in which it is formed, and its size decreases exponentially with time (Figure 2b). During the process, the cylindrical hydrogel is always anchored to the air/water interface, probably due to the increased hydrophobicity of the microgel particles at high temperatures; this leads to a stronger adhesion to the hydrophobic air/water interface than to the more hydrophilic glass walls of the

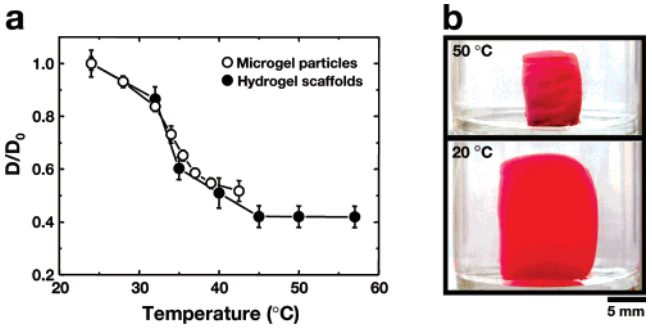

Figure 3. (a) Deswelling behavior of the single microgel particle and the hydrogel scaffold. We plot the diameter, D, normalized by the initial diameter, D_0, as a function of the temperature, T. Particle diameters of the microgel particles were measured by using dynamic light scattering (HS4500, Malvern). (b) A hydrogel scaffold before and after the transition temperature. In this case, the microgel particles were copolymerized with rhodamine-tagged monomers (Polyfluor 570, ~0.05 wt %, Polysciences) to achieve better visualization. The system reversibly changed between these two states.

container.[34,35] By contrast, when the scaffold is fabricated in plastic containers, such as polyethylene and polypropylene, it always adheres to both the air/water interface and the container walls, inhibiting the formation of the desired structure. Thus some hydrophilicity of the container walls is essential in our technique; in this case, the shape of the container completely determines the shape of the scaffold. For instance, if cubic containers of glass are used instead of cylindrical containers of glass, cubic hydrogels are generated. Our procedure thus provides great flexibility in designing the shape of the hydrogel structure.

Once this structure is fabricated, it maintains the thermal sensitivity of the single microgel particles, as shown in Figure 3a. Both microgel particles and hydrogel scaffolds show an equivalent decrease in size, when normalized by the low-temperature dimensions, with increasing temperature. They also exhibit a transition temperature of ~32 °C, typical of PNIPAm gels and microgels, and lack any size hysteresis after repeated heating and cooling cycles (Figure 3b). These results demonstrate that the thermal properties of the hydrogel scaffold are determined solely by those of its unit building blocks; this adds further flexibility to our technique, as fine-tuning of the microgel properties enables manipulation of the properties of the hydrogel scaffolds that are made with them.

Our hydrogel structure exhibits a remarkable improvement in response dynamics. In conventional polymer gels, the time to deswell is determined by the polymer relaxation time,[21,22] τ, which characterizes the decay of size in time: $D(t) = (A - A_f)e^{(-t/\tau)} + A_f$; $D(t)$ is the gel diameter at time t in the case of cylindrical gels, A is the initial size, and A_f is the final size. To illustrate this improvement, we fabricate a bulk hydrogel using the same chemistry as the microgel particles and the same size as our hydrogel scaffolds and plot the evolution of the size after a sudden temperature jump from 20 to 44 °C (Figure 4a). The size decreases exponentially with time until the final deswollen dimensions are approached. From the data, we obtain $\tau_{bulk} \sim 1.5 \times 10^4$ s, which is consistent with previous studies.[22,23] For our hydrogel scaffold, we obtain a similar temporal evolution of the size but with $\tau_{scaffold} \sim 1.4 \times 10^2$ s (Figure 4b), which is $\sim 10^2$ times smaller than τ_{bulk}. The reswelling of this hydrogel scaffold after a sudden temperature jump from 44 to 20 °C is characterized by a similar relaxation time, $\tau_{scaffold} \sim 1.5 \times 10^2$ s, and an identical original dimension. These remarkably faster kinetics arise from the small dimensions of the microgel particles that form the scaffold structure; the smaller size speeds the diffusion of fluid through the microgel particles, thereby reducing τ. Nevertheless, this time is still larger than the deswelling time of a single microgel particle, which is ~10 ms;[36] this is most likely due to the covalent bonds that are established among the microgel particles that affects their own relaxation time and reduces the overall permeability of the scaffold by comparison to a single microgel particle. We further note that the enhanced kinetics of our scaffolds are achieved without significant loss in mechanical strength, an essential feature for applications. We have obtained a compressive modulus of 5×10^3 Pa at 20 °C and 1.1×10^5 Pa at 44 °C to be compared with $\sim 10^4$ Pa at 20 °C and $\sim 10^5$ Pa at 44 °C that are typical for bulk hydrogels.[37]

The robustness of our fabrication technique enables hybridization of a wide variety of materials within the responsive hydrogel scaffold. We demonstrate this by

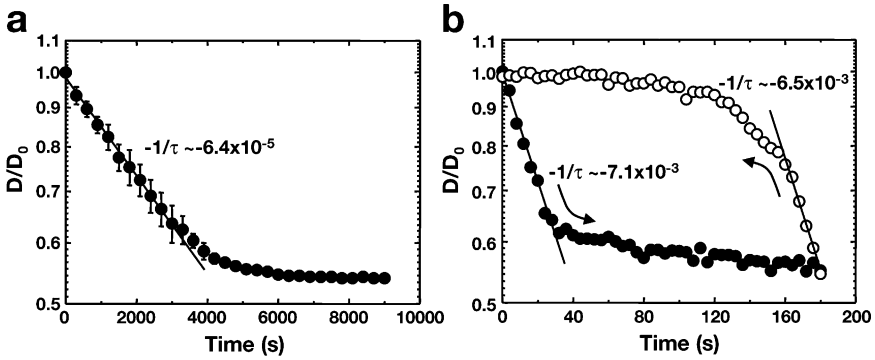

Figure 4. Time evolution of the swelling ratio, $D(t)/D_0$, for (a) a bulk hydrogel and (b) a hydrogel scaffold, where D_0 is the initial size. From the exponential fits shown in the graphs, we obtained the characteristic deswelling time for both structures. In these measurements, the samples were first allowed to equilibrate at 20 °C for 24 h and were subsequently introduced inside a water bath, whose temperature was precisely set to 44 °C. To determine the reswelling time of the hydrogel scaffold shown in panel b, the same sample was equilibrated at 44 °C and then was swelled at 20 °C, following the same procedure used for determining the deswelling time.

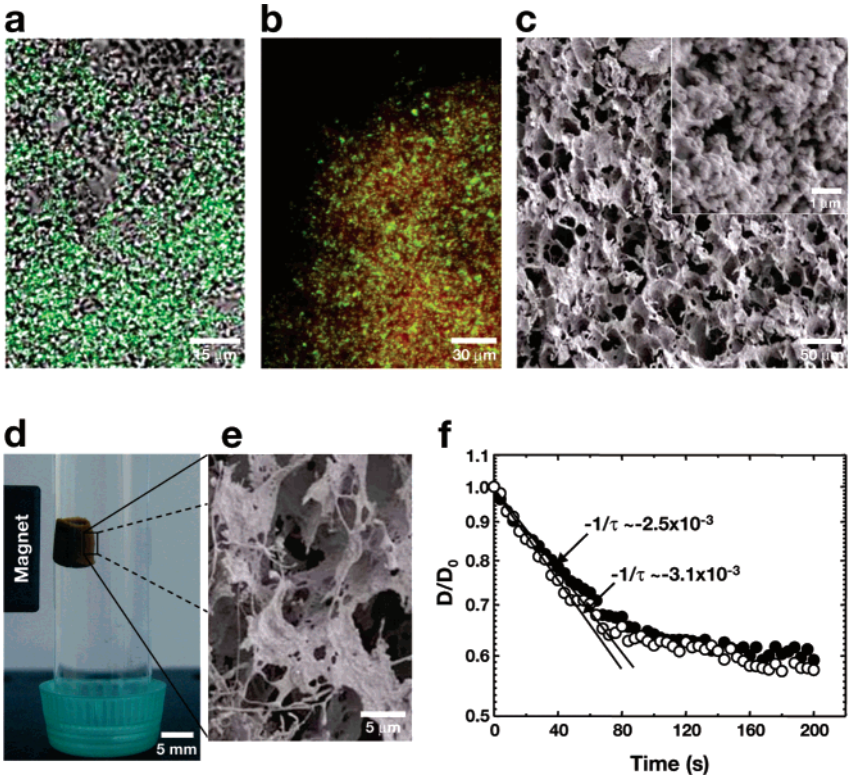

Figure 5. Hybridization of the hydrogel scaffolds with a variety of functional materials. (a) A differential interference contrast image for a hydrogel scaffold immobilizing the antibody fluorescein-conjugated goat antimouse immunoglobulin G. Approximately 1% w/v antibody was formulated in the original microgel dispersion. (b) A fluorescence image of a scaffold hybridized with fluorescein-labeled polystyrene particles (1 μm, NH_2 functionalized, green, ~0.1% w/v, Invitrogen). In this case, the microgel particles were labeled with Polyfluor 570 (~0.01 wt %, red). (c) A scanning electron microscope (SEM) image of a hydrogel scaffold hybridized with silica particles (~200 nm, 0.2% w/v, Ludox HS40, Aldrich). (d,e) Hydrogel scaffolds hybridized with magnetic nanoparticles (~10 nm, ~0.1 vol %, EMG 607, FerroTec). The SEM photographs were taken after freeze-drying the samples. (f) Time evolution of the swelling ratio for hybridized hydrogel scaffolds with silica particles (closed circles, ~200 nm, 0.2% w/v) and magnetic nanoparticles (open circles, ~10 nm, ~0.1 vol %). In these measurements, we equilibrated the samples at 20 °C and deswelled them at 44 °C.

engineering the hydrogels with several representative functional materials. The hydrogel scaffold serves as a thermally responsive reservoir for these additional components. For example, we have homogeneously immobilized antibody proteins and fluorescein-conjugated goat antimouse immunoglobulin G within the hydrogel scaffold (Figures 5a). We have also engineered composite hydrogels by hybridizing fluorescently labelled polystyrene particles (Figure 5b), silica particles (Figure 5c), and magnetic nanoparticles (Figure 5d,e). This hybridization occurs irrespective of the surface properties of the added particles. In the case of positively charged colloidal materials, we take advantage of the electrostatic attraction between these species and the negatively charged groups of the PAAc to induce adhesion to the microgel particles. By contrast, when the colloidal materials have either negative or no charge, we use the depletion interaction to induce aggregation with the microgel particles[38] (see Supporting Information). In this fashion, we have fabricated magnetic composite hydrogels with either negatively or positively charged magnetic nanoparticles. Notably, the added colloidal particles, regardless of the size and type, remain within the hydrogel matrix even after repeated heating and cooling cycles, implying that they have been structurally locked in the microgel structure. Even after the hybridization process, the composite hydrogels maintain their excellent thermo-sensitivity as well as their fast response time, as shown in Figure 5f. We obtain $\tau_{scaffold-silica} \sim 4.0 \times 10^2$ s and $\tau_{scaffold-Fe_2O_3} \sim 3.2 \times 10^2$ s for scaffolds containing silica and magnetic particles, respectively. Moreover, they display the functions that originate from the added materials (see Supporting Information).

In conclusion, this study introduces a framework for fabricating hydrogel scaffolds that exhibit fast response kinetics and the important ability of retaining a variety of functional materials without affecting the original functions of both the building blocks of the scaffold and the added species. The key to our approach is the use of submicron microgel particles that can be assembled either through bridging or depletion interactions to yield a structure that swells or deswells at a macroscopic level in much shorter times as compared to a bulk polymer gel of similar characteristics. Future studies will focus on achieving scaffolds with denser packings of microgel particles that should have even higher mechanical strength compared to those presented in this study. The approach we have presented offers a new way of fabricating robust and functional hydrogel scaffolds with excellent loading capabilities for a wide variety of materials, irrespective of chemistry, size, and shape. Moreover, these materials are controllable and responsive to external stimuli.

Acknowledgment. This work was supported by the Postdoctoral Fellowship Program of Korea Research Foundation (KRF), Amore-Pacific Co. R&D Center in Korea, the NSF (DMR-0602684), and the Harvard MRSEC (DMR-0213805). A.F.-N. is grateful to Junta de Andalucia (FQM-3116) and to University of Almeria (leave of absence).

Supporting Information Available: Detailed experimental methods. Fabrication of hydrogel scaffolds by using the depletion interactions (Figure S1). A movie for the fabrication of hydrogel scaffolds (Movie S1). A movie for the response of a magnetically hybridized hydrogel scaffold to magnetic field gradients (Movie S2). This material is available free of charge via the Internet at http://pubs.acs.org.

References

(1) Tanaka, T. *Phys. Rev. Lett.* **1978**, *40*, 820−823.
(2) Hirokawa, Y.; Tanaka, T. *J. Chem. Phys.***1984**, *81*, 6379−6380.
(3) Kwon, I. C.; Bae, Y. H.; Kim, S. W. *Nature* **1991**, *354*, 291−293.
(4) Suzuki, A.; Tanaka, T. *Nature* **1990**, *346*, 345−347.
(5) Juodkazis, S.; Mukai, N.; Wakaki, R.; Yamaguchi, A.; Matsuo, S.; Misawa, H. *Nature* **2000**, *408*, 178−181.
(6) Ikeda, T.; Nakano, M.; Yu, Y.; Tsutsumi, O.; Kanazawa, A. *Adv. Mater.* **2003**, *15*, 201−205.
(7) Lendlein, A.; Jiang, H.; Junger, O. *Nature* **2005**, *434*, 879−882.
(8) Miyata, T.; Asami, N.; Uragami, T. *Nature* **1999**, *399*, 766−769.
(9) Pelton, R. *Adv. Colloid Interf. Sci.* **2000**, *85*, 1−33.
(10) Lindman, S.; Lynch, I.; Thulin, E.; Nilsson, H.; Dawson, K. A.; Linse, S. *Nano Lett.* **2007**, *7*, 914−920.
(11) Zhang, Y.; Guan, Y.; Zhou, S. *Biomacromolecules* **2007**, *7*, 3196−3201.
(12) Reese, C. E.; Mikhonin, A. V.; Kamenjicki, M.; Tikhonov, A.; Asher, S. A. *J. Am. Chem. Soc.* **2004**, *126*, 1493−1496.
(13) Koholek, M.; Lee, W. K.; LaMattina, B.; Caster, K. C.; Zauscher, S. *Nano Lett.* **2004**, *4*, 373−376.
(14) Kim, J.; Nayak, S.; Lyon, L. A. *J. Am. Chem. Soc.* **2005**, *127*, 9588−9592.
(15) Debord, J. D.; Lyon, L. A. *J. Phys. Chem. B* **2000**, *104*, 6327−6331.
(16) Hu, Z.; Huang, G. *Angew. Chem., Int. Ed.* **2003**, *42*, 4799 −4802.
(17) Nyak, S.; Lee, H.; Chmielewski, J.; Lyon, L. A. *J. Am. Chem. Soc.* **2004**, *126*, 10258−10259.
(18) Gorelikov, I.; Field, L.; Kumacheva, E. *J. Am. Chem. Soc.* **2004**, *126*, 15938−15939.
(19) Tanaka, T.; Fillmore, D. J. *J. Chem. Phys.* **1979**, *70*, 1214−1218.
(20) Matsuo, E. S.; Tanaka, T. *J. Chem. Phys.* **1988**, *89*, 1695−1703.
(21) Okajima, T.; Harada, I.; Nishio, K.; Hirotsu, S. *J. Chem. Phys.* **2002**, *116*, 9068−9077.
(22) Li, Y.; Wang, G.; Hu, Z. *Macromolecules* **1995**, *28*, 4194−4197.
(23) Bansil, R.; Liao, G.; Falus, P. *Physica A* **1996**, *231*, 346−358.
(24) Dong, L. C.; Hoffman, A. S. *J. Controlled Release* **1990**, *13*, 12−31.
(25) Zhang, X. Z.; Yang, Y. Y.; Chung, T. S.; Ma, K. X. *Langmuir* **2001**, *17*, 6094−6099.
(26) Kuang, M.; Wang, D.; Gao, M.; Hartmann, J.; Mohwald, H. *Chem. Mater.* **2005**, *17*, 656−660.
(27) Yoshida, R.; Uchida, K.; Kaneko, Y.; Sakai, K.; Kikuchi, A.; Sakurai, Y.; Okano, T. *Nature* **1995**, *374*, 240−242.
(28) Kaneko, Y.; Nakamura, S.; Sakai, K.; Aoyagi, T.; Kikuchi, A.; Sakurai, Y.; Okano, T. *Macromolecules* **1998**, *31*, 6099−6105.
(29) van Durme, K.; van Mele, B.; Loos, W.; du Prez, F. E. *Polymer* **2007**, *46*, 9851−9862.
(30) Petit, L.; Bouteiller, L.; Brulet, A.; Lafuma, F.; Hourdet, D. *Langmuir* **2007**, *23*, 147−158.
(31) Larson, R. G. *The Structure and Rheology of Complex Fluids*; Oxford University Press: New York, 1998.
(32) Ohshima, H. *Adv. Colloid Interf. Sci.* **1994**, *53*, 77−102.
(33) Huang, G.; Hu, Z. *Macromolecules* **2007**, *40*, 3749−3756.
(34) Ngai, T.; Auweter, H.; Behrens, S. H. *Macromolecules* **2006**, *23*, 8171−8177.
(35) Ngai, T.; Behrens, S. H.; Auweter, H. *Chem. Commun.* **2005**, *3*, 331−333.
(36) Hoare, T.; Pelton, R. *J. Phys. Chem. B* **2007**, *111*, 1334−1342.
(37) Muniz, E. C.; Geuskens, G. *Macromolecules* **2001**, *34*, 4480−4484.
(38) Tuinier, R.; Rieger, J.; de Kruif, C. G. *Adv. Colloid Interf. Sci.* **2003**, *103*, 1−31.

NL072346E